LETTER

doi:10.1038/nature12718

Themis sets the signal threshold for positive and negative selection in T-cell development

Guo Fu[1], Javier Casas[1,2]*, Stephanie Rigaud[1]*, Vasily Rybakin[1,2]*, Florence Lambolez[3], Joanna Brzostek[1,2], John A. H. Hoerter[1], Wolfgang Paster[4], Oreste Acuto[4], Hilde Cheroutre[3], Karsten Sauer[1,5] & Nicholas R. J. Gascoigne[1,2]

Development of a self-tolerant T-cell receptor (TCR) repertoire with the potential to recognize the universe of infectious agents depends on proper regulation of TCR signalling. The repertoire is whittled down during T-cell development in the thymus by the ability of quasi-randomly generated TCRs to interact with self-peptides presented by major histocompatibility complex (MHC) proteins. Low-affinity TCR interactions with self-MHC proteins generate weak signals that initiate 'positive selection', causing maturation of CD4- or CD8αβ-expressing 'single-positive' thymocytes from $CD4^+CD8\alpha\beta^+$ 'double-positive' precursors[1]. These develop into mature naive T cells of the secondary lymphoid organs. TCR interaction with high-affinity agonist self-ligands results in 'negative selection' by activation-induced apoptosis or 'agonist selection' of functionally differentiated self-antigen-experienced T cells[2,3]. Here we show that positive selection is enabled by the ability of the T-cell-specific protein Themis[4–9] to specifically attenuate TCR signal strength via SHP1 recruitment and activation in response to low- but not high-affinity TCR engagement. Themis acts as an analog-to-digital converter translating graded TCR affinity into clear-cut selection outcome. By dampening mild TCR signals Themis increases the affinity threshold for activation, enabling positive selection of T cells with a naive phenotype in response to low-affinity self-antigens.

Themis-deficient mice have severely reduced numbers of single-positive thymocytes and peripheral T cells[4–8], but the mechanism by which Themis controls T-cell development or function remains obscure. Its rapid phosphorylation after TCR stimulation[4,9,10] and subtle signalling defects in *Themis*$^{-/-}$ double-positive thymocytes suggested a role in proximal TCR signalling[4,9,11], although others failed to find any alteration in TCR signalling[5–7,10]. Such mild or undetected signalling defects seemed incompatible with the strong positive selection defect in Themis-deficient mice.

We suspected that activation by antibody-mediated TCR crosslinking may have masked genuine signalling defects that would be revealed with more physiological stimulation. Calcium flux is a hallmark of early TCR signalling and is very sensitive to differences in signal strength[12]. We titrated streptavidin crosslinking for anti-CD3/CD4 antibodies to better mimic graded signal strengths TCRs might generate *in vivo*. Over a broad concentration range, we found only minor reduction in calcium signal in Themis-deficient thymocytes, consistent with our previous observations[4], but of dubious biological relevance (Extended Data Fig. 1). Therefore, we used the well-characterized OT-I TCR-transgenic model[13] to enable thymocyte activation by more physiological MHC proteins ligands. Natural positively selecting and antigen-variant peptides eliciting a full spectrum of signal strengths are well documented (Extended Data Fig. 2a). OT-I *Tap1*$^{-/-}$ mice express low cell-surface MHC-I, so thymocyte development is arrested at the pre-selection double-positive stage. Therefore OT-I *Tap1*$^{-/-}$*Themis*$^{-/-}$ or *Themis*$^{+/+}$ thymocytes are an excellent system to study TCR signalling after stimulation with appropriate antigen H-2K^b (K^b) tetramers. As expected, Themis-sufficient double-positive thymocytes gave very low but sustained Ca^{2+} responses to positively selecting peptides Q4H7, Q7 and G4[12]. Remarkably, Themis-deficient cells responded much stronger than Themis-sufficient cells to these ligands, also giving increased responses to lower-affinity E1 and the natural positive-selector Catnb. Responses to strong agonists OVA (the antigenic peptide for OT-I T cells) and its variant A2 (see Extended Data Fig. 2a) were similar between genotypes (Fig. 1a–c and Extended Data Fig. 2b). Similar results were obtained by stimulation on supported lipid bilayers (Fig. 1d). These results were confirmed by imaging Ca^{2+} in thymocytes recognizing RMA-S cells presenting representative high (OVA)- or low (G4)-affinity peptides. Themis-deficient thymocytes responded more strongly than Themis-sufficient to G4, but similarly to OVA (Fig. 1e, f and Extended Data Fig. 3). The strong, transient Ca^{2+} response to negative-selecting ligands versus low, sustained signal to positively selecting ligands[12], are reflected in differential nuclear translocation of NFATC2[14]. Themis-sufficient thymocytes induced strong, transient NFATC2 translocation in response to K^b–OVA tetramer, and delayed but more sustained translocation in response to K^b–G4 (Fig. 1g, Extended Data Fig. 4). In contrast, in Themis-deficient thymocytes, both K^b–OVA and K^b–G4 tetramers induced nearly identical NFATC2 translocation kinetics, similar to the K^b–OVA response of wild-type thymocytes. These data demonstrate that the role of Themis in thymocyte signalling is manifest in the response to weak ligands, but masked in responses to strong (agonist) ligands. These differences were largest with ligands below the previously described positive-negative selection border[12]. Differences were noticeable for ligands slightly above this threshold (weak agonists), but were completely masked by antibody crosslinking.

Appropriate ERK signalling kinetics are critical for positive selection[15–17]. As shown previously, antibody crosslinking induced slightly weaker ERK phosphorylation in Themis-deficient compared to Themis-sufficient cells[4] (Extended Data Fig. 5). Further analysis of phosphorylated (p)-ERK by flow cytometry showed roughly equal p-ERK responses induced with K^b–OVA tetramer in both genotypes. However, ERK signalling was faster and stronger in Themis-deficient double-positive cells in response to ligands weaker than K^b–OVA (Fig. 2a, b and Extended Data Fig. 6), and confirmed by immunoblot (Extended Data Fig. 5). These data further support the notion that *Themis*$^{-/-}$ cells receive signals induced by classical positive-selecting ligands as activating signals, similar to negative/agonist ligand-induced signals.

The subcellular localization of p-ERK in thymocytes differs with ligand affinity, with negative/agonist-selection stimuli inducing p-ERK more proximal to the plasma membrane than positive-selection stimuli, which induced p-ERK deeper within the cell[12]. To determine whether Themis controls the topology of TCR-induced ERK activation, we

[1]Department of Immunology and Microbial Science, The Scripps Research Institute, 10550 North Torrey Pines Road, La Jolla, California 92037, USA. [2]Department of Microbiology, Yong Loo Lin School of Medicine and Immunology Programme, National University of Singapore, 5 Science Drive 2, Singapore 117545. [3]Developmental Immunology, La Jolla Institute for Allergy and Immunology, 9420 Athena Circle, La Jolla, California 92037, USA. [4]Sir William Dunn School of Pathology, University of Oxford, South Parks Road, Oxford OX1 3RE, UK. [5]Department of Cell and Molecular Biology, The Scripps Research Institute, 10550 North Torrey Pines Road, La Jolla, California 92037, USA.
*These authors contributed equally to this work.

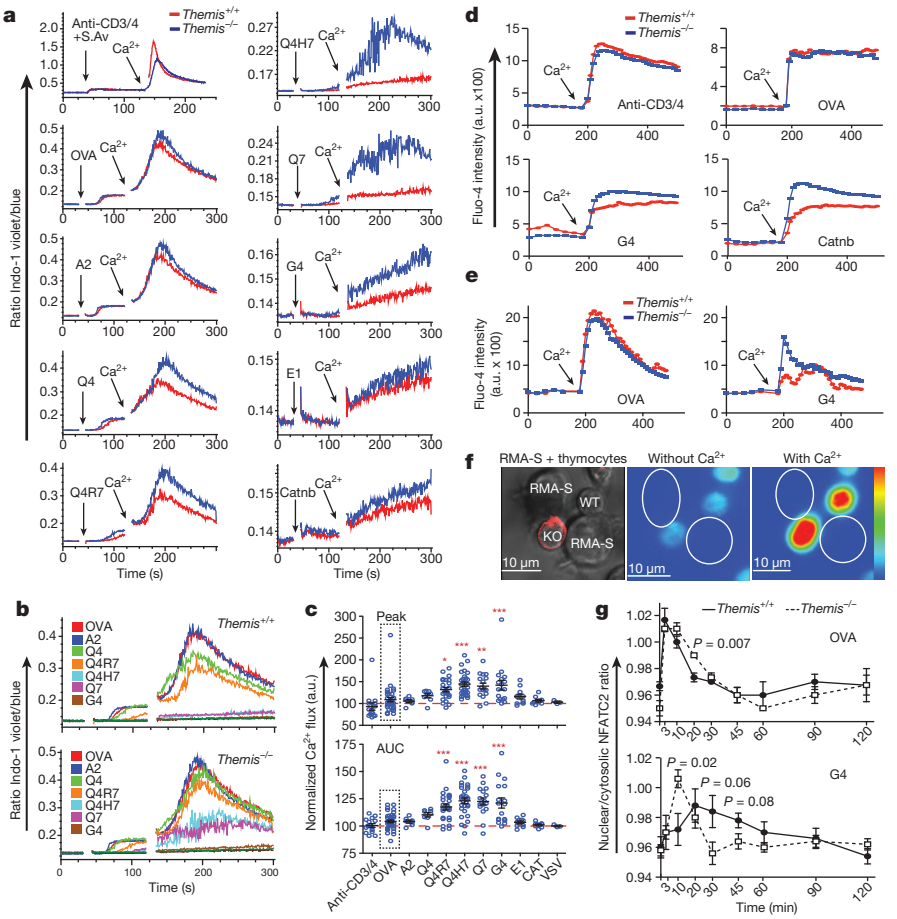

Figure 1 | Differentially regulated Ca^{2+} flux in *Themis*$^{-/-}$ thymocytes. **a**, **b**, *Themis*$^{+/+}$ or *Themis*$^{-/-}$ OT-I pre-selection thymocytes were incubated with indicated stimuli. Results of representative experiment shown in **a**, same-genotype comparisons in **b**. **c**, Summary of Ca^{2+} flux differences. Each dot represents one *Themis*$^{-/-}$ sample normalized to its same-tube *Themis*$^{+/+}$ control[30] (sex and age-matched), thus blinding and randomization was unnecessary. Each paired sample represents a biological and technical replicate[30]. Data obtained from eight litters of each genotype over 10 months. Peak-height (top) and area-under-the-curve (AUC, bottom) shown. Statistical significance determined by one-way analysis of variance Dunnett's test, with OVA as comparison control. $*P < 0.05$, $**P < 0.01$, $***P < 0.001$. Minimal sample size needed to obtain $P = 0.05$, 90% power, estimated based on 1.2-fold difference. a.u., arbitrary units. **d**, Ca^{2+} flux imaging on supported lipid bilayers. Cells settled on K^b-monomer or antibody-coated lipid bilayer were imaged before and after adding $CaCl_2$. Graphs show mean Fluo-4 intensity (wild type (WT): $n = 11, 27, 17, 29$; KO: $n = 20, 14, 24, 23$, for cells stimulated by antibody, OVA, G4 and Catnb, respectively), representative of two experiments. **e**, Live Ca^{2+} imaging of stimulation by RMA-S cells pre-loaded with OVA ($n = 5$) or G4 ($n = 8$) peptide, measured as in **d**. Representative of three experiments. **f**, Representative images of OVA-stimulation of cells analysed in **e**. *Themis*$^{-/-}$ cells identified by Cy5 staining (red on transmitted light image), Ca^{2+} scale on right. **g**, NFATC2 translocation in thymocytes responding to K^b–OVA and K^b–G4 tetramers. Nuclear/cytosolic NFATC2 protein ratios (Extended Data Fig. 4) calculated using CellProfiler, $n = 70$ cells per data-point. Mean ± s.e.m. shown. P values from unpaired t-test. Representative of two experiments.

compared p-ERK localization in Themis-deficient or Themis-sufficient pre-selection double-positive thymocytes responding to different ligands (Fig. 2c, d and Extended Data Fig. 7). Weak ligands that normally induce intracellular p-ERK in Themis-expressing cells instead gave a relatively high proportion of membrane-proximal p-ERK in *Themis*$^{-/-}$ DPs. In aggregate, these data indicate that, without Themis, the ERK cascade

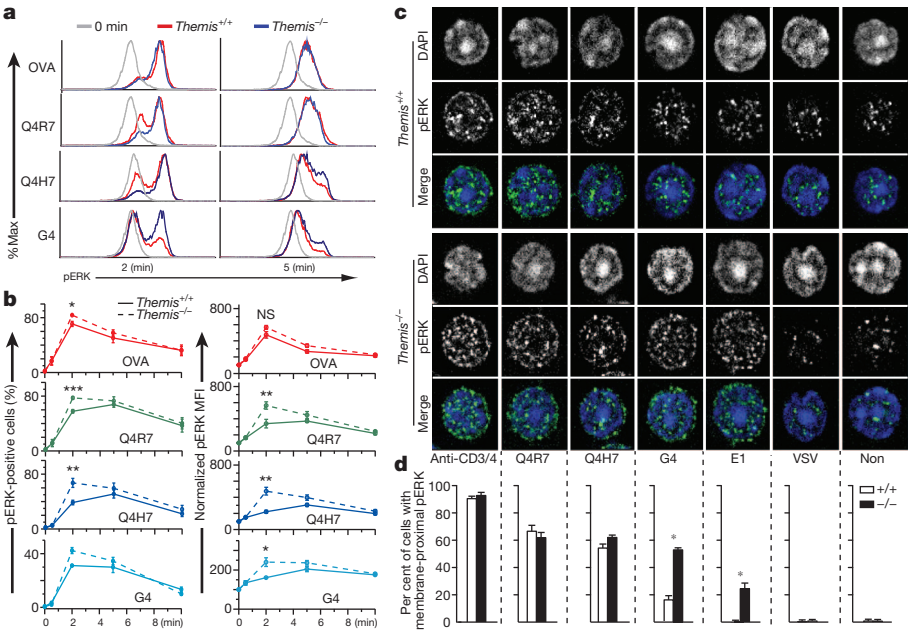

Figure 2 | Themis-deficiency allows low-affinity ligands to elicit negative selection-like characteristics of ERK activation. Themis-sufficient or Themis-deficient pre-selection thymocytes were stimulated with K^b-tetramers. **a**, **b**, ERK phosphorylation detected by flow cytometry following intracellular staining. Representative FACS plots shown in **a** and Extended Data Fig. 6. %Max, per cent of maximum. **b**, Summarized data compiled from multiple experiments ($n = 5$ for OVA, Q4R7 and Q4H7, $n = 8$ for G4), presented as mean ± s.e.m. of percentage p-ERK$^+$ cells (left), MFI, mean fluorescence intensity (right). Sample sizes estimated as Fig. 1. $*P < 0.05$, $**P < 0.01$ and $***P < 0.001$, paired t-test. **c**, **d**, Localization of p-ERK determined by staining stimulated thymocytes (2 min) with DAPI and anti-p-ERK[12]. **c**, Representative images. **d**, Percentage of cells with membrane-proximal p-ERK, $n = 20$ for each condition, mean ± s.e.m. Representative of four experiments for each tetramer, two different operators, not blinded. Unpaired t-test on two identical experiments, $*P < 0.05$.

was both mis-localized and hyperactivated, so that positive-selecting ligands were mistakenly interpreted as negative/agonist-selectors. Thus, *Themis*$^{-/-}$ double-positive cells seem unable to precisely distinguish low-affinity from high-affinity TCR signalling.

Both the Ca^{2+} response and ERK signalling cascade occur distal to TCR stimulation. We therefore examined more proximal signalling events to determine where these marked changes in signal transduction to low-affinity ligands were initiated. We found substantially elevated phosphorylation of LAT and PLCγ1 (Fig. 3a), although not SLP-76 (Extended Data Fig. 8), in Themis-deficient versus Themis-sufficient cells upon stimulation with low-affinity ligands. This point of action is consistent with previous reports that Themis interacts with PLCγ1 and is part of the LAT signalosome[4,9,11]. These data demonstrate that *Themis*$^{-/-}$ cells mount an augmented response to low-affinity ligands, similar to a wild-type response to high-affinity ligands, indicating that Themis restricts TCR signalling in double-positive cells stimulated by low-affinity ligands. SHP1, a cytoplasmic protein tyrosine phosphatase, is an important negative regulator in TCR signalling (reviewed in ref. 18). It is activated by tyrosine phosphorylation, and reported to control the thresholds for positive and negative selection[18–21]. To test if Themis might limit TCR signalling by controlling SHP1, we analysed SHP1 phosphorylation in *Themis*$^{+/+}$ and *Themis*$^{-/-}$ double-positive cells. Notably, p-SHP1 (but not total protein) was markedly decreased in Themis-deficient cells, clearly opposite to enhanced p-ERK. Indeed p-SHP1 was barely induced in the Themis-deficient cells (Fig. 3b and Extended Data Fig. 9). Moreover, Themis interacted constitutively with SHP1 but p-SHP1 was induced in Themis-SHP1 complexes in response to TCR stimulation (Fig. 3c). Themis–GRB2 binding was constitutive (Fig. 3d)[5–7,9]. Because activated LCK is a SHP1 substrate[18,22], we tested LCK phosphorylation, finding that the activated pY394 form was indeed increased in Themis-deficient thymocytes (Fig. 3e).

These results suggest that Themis 'caps' the signal strength by controlling SHP1 activation, moderating strength and kinetics of responses to relatively low-affinity ligands. This allows these self-antigen-experienced cells to mature into naive T cells. Without Themis, thymocytes receive strong agonist/negative-selection-like signals. To test whether these redirect low-affinity stimulation to induce negative selection, we stimulated pre-selection double-positive thymocytes with K^b-tetramers, and assayed caspase-3 activation, a readout for apoptosis[23]. Indeed, caspase-3 activation was significantly increased in *Themis*$^{-/-}$ versus *Themis*$^{+/+}$ cells in response to ligands that normally induce positive selection, but was similar for ligands that normally induce negative selection (Fig. 4a, left). Reduced activated caspase-3$^+$ cells in OVA-stimulated populations versus weaker ligands is probably due to phagocytosis of dead cells, as OVA signals were clearly stronger based on TCR downmodulation (Fig. 4a, right). Deficiency of the pro-apoptotic protein Bim rescues thymocytes from negative selection[24]. Intriguingly, *Bim* co-disruption rescued the previously reported[4–8] impaired single-positive thymocyte development in *Themis*$^{-/-}$ mice and defective CD8SP thymocyte development in OT-I *Themis*$^{-/-}$ mice (Fig. 4b, c). This indicated that the defect in thymocyte development in *Themis*$^{-/-}$

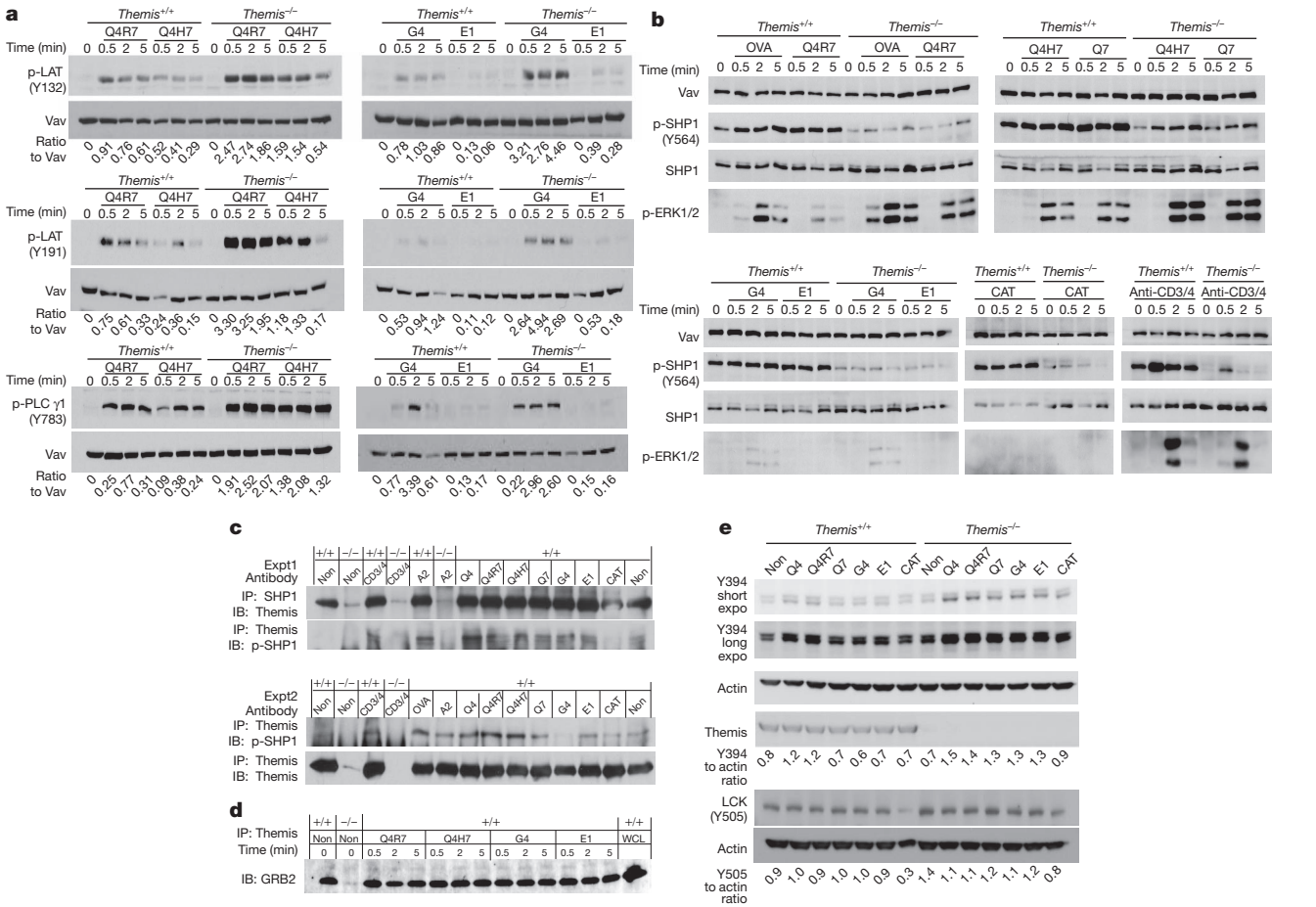

Figure 3 | Proximal TCR signalling in Themis-deficient thymocytes responding to positive selecting ligands. *Themis* KO or WT pre-selection thymocytes were stimulated with indicated tetramers and analysed by immunoblot. **a**, LAT and PLCγ1 phosphorylation. **b**, SHP1 and ERK1/2 phosphorylation. Vav was used as loading control. **c**, Themis interaction with SHP1 and p-SHP1 (Expt, experiment). **d**, Themis interaction with GRB2. IB, immunoblot; IP, immunoprecipitation. **e**, Phosphorylation of LCK in response to different stimuli. The lower molecular weight band in blots probed with anti-p-Y394 is LCK (p56), the higher is FYN (p59). expo, exposure. Representative of 2 (**b**), 3 (**a**, **c**, **e**) and 6 (**d**) experiments, respectively.

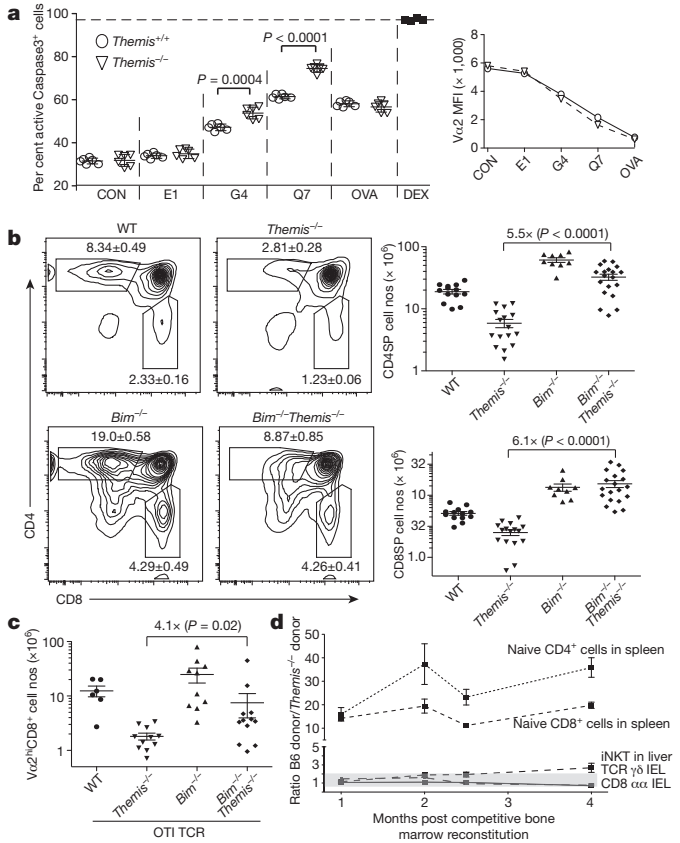

Figure 4 | Themis-deficient mice show enhanced negative selection that can be rescued by Bim deficiency, but normal agonist selection. **a**, Pre-selection thymocytes were stimulated with tetramers for 17 h, then analysed for activated caspase-3[23]. Triplicate measurements for two mice per genotype, showing mean ± s.e.m. Right panel shows TCR down-modulation. Representative of 3 experiments. **b**, Thymocytes were analysed for CD4 and CD8 expression. 4–6-week-old mice of both sexes included, no randomization nor blinding necessary for genetic experiment read by flow cytometry. Sample sizes chosen to obtain $P = 0.01$, 90% power for fivefold difference. Left, representative plots showing mean ± s.e.m. percentage of each subset labelled. Right, summarized data of absolute numbers for each subset. **c**, Mice of indicated genotypes as **b** but expressing OT-I TCR-transgene, analysed for $V\alpha2^{hi}CD8^{+}$ subset. Summarized data of absolute cell numbers shown. In **b** and **c**, each symbol represents a single mouse. Statistics, unpaired *t*-test (**a**) and Mann–Whitney test (**b**, **c**). Fold increases and *P* values between indicated samples shown in each scheme. **d**, Phenotypic analysis of indicated subsets in competitive bone-marrow-reconstituted mice. Data pooled from multiple experiments, shown as mean ± s.e.m. after normalizing $Themis^{+/+}$-derived donor cells to $Themis^{-/-}$ donor cells ($n = 4$ pairs of mice per time point except 2 months, 8 pairs). Grey zone indicates ratio between 0.5 and 2. Group sizes based on prior experience.

mice is caused at least partially by misplaced negative selection (agonist selection would not be affected by Bim-deficiency). This suggested the possibility that, although conventional naive T-cell development requiring weak sustained signalling is severely impaired, agonist-selection of non-conventional T cells by intermediate affinity ligands might be spared or compensated in Themis-deficient mice. To test this, we simultaneously examined development of wild-type and Themis-deficient T cells in mixed bone marrow chimaeras, avoiding potential homeostatic proliferation artefacts (Fig. 4d). $Themis^{+/+}$ vastly outnumbered $Themis^{-/-}$ cells among conventionally selected naive peripheral T cells, but $TCR\gamma\delta^{+}$ intra-epithelial lymphocytes (IEL), $TCR\alpha\beta^{+}$ $CD8\alpha\alpha$ IELs and liver iNKT-cells, which all are selected from double-positive cells by strong TCR signals[2,3,25], showed roughly equal reconstitution by both genotypes. Thus, development of agonist-selected T cells is not, or at most very mildly, affected by the absence of Themis, in contrast to generation of peripheral naive T cells, supporting our notion that the role of Themis differs in relation to ligand strength.

This study shows that Themis acts early in the TCR signalling cascade, reducing signal strength in response to low-affinity but not high-affinity MHC proteins ligands. Without Themis, TCR signalling in response to low-affinity MHC proteins ligands mimics normal signalling responses to negative or agonist-selecting ligands, generating stronger signals that redirect the selection outcome. Themis performs this function through controlling recruitment and activation of the phosphatase SHP1, which limits TCR signalling and reportedly affects the thresholds for positive and negative selection[19–21], as well as helping discriminate between agonist and lower-affinity antagonist ligands[22]. A recent study using a conditional knockout of SHP1, where deletion occurred at the immature double-positive stage of thymocyte development, showed that SHP1 was not required for normal thymocyte development[26]. It is possible that incomplete deletion of SHP1 mediated by transgenic CD4-Cre may mask the requirement of SHP1 in thymocyte development. Alternatively other phosphatases can act redundantly in selection[26]. The dominant negative SHP1 transgenes that appeared to show the involvement of SHP1 in development[19,20] would likely have blocked other phosphatases in addition to SHP1. We therefore tested whether Themis is able to interact with SHP2. We found that Themis indeed interacts constitutively with SHP2 (Extended Data Fig. 10), indicating that the lack of a $Themis^{-/-}$-like phenotype in the conditional SHP1 knockout is probably owing to redundancy between phosphatases, raising the possibility that different phosphatases may be important in TCR signalling in different situations.

Themis acts to enforce the threshold between positive and negative/agonist selection, which occurs over a very narrow range of TCR–MHC protein affinities[12]. Themis causes an analog continuum of TCR affinities to elicit a digital selection outcome—positive versus negative/agonist selection. We speculate that altered Themis expression shifts the selection window, changing the mature TCR repertoire, and therefore affecting disease susceptibility. Indeed, single-nucleotide polymorphisms in the noncoding region between human *THEMIS* and *PTPRK* genes have been associated with susceptibility to coeliac disease and multiple sclerosis[27–29]. More work is needed to understand the connection between these polymorphisms, Themis expression and the aetiology of disease.

METHODS SUMMARY

Animal experiments were performed in accordance with the TSRI Animal Care and Use Committee. Thymocytes from $Themis^{+/+}$ or $Themis^{-/-}$ OT-I $Tap1^{-/-}$ 4–6-week-old mice, both sexes, were used. For *ex vivo* experiments, thymocytes were rested 3 h at 37 °C before assay. For Ca^{2+} assays, knockout cells were pre-labelled with Cy5 and mixed with wild-type cells (or vice versa), loaded with Ca^{2+}-sensitive dye (indo-1-AM for flow cytometry or Fluo-4 for imaging), then washed in Ca^{2+}/Mg^{2+}-free medium, 1 mM EGTA[30]. Cells were stimulated with tetramers for flow cytometry[30], or with antigen-presenting lipid bilayers or peptide-loaded RMA-S cells for imaging. After allowing cells to settle, 1 v/v pre-warmed medium containing 2.5 mM $CaCl_2$ and $MgCl_2$ was added ($t = 0$). For biochemistry, thymocytes were stimulated with tetramers or antibodies, and analysed by western blot as described[4,12]. Rabbit anti-Themis antibody (Millipore 06-1328) was used in immunoprecipitation and blotting.

Online Content Any additional Methods, Extended Data display items and Source Data are available in the online version of the paper; references unique to these sections appear only in the online paper.

Received 26 February; accepted 26 September 2013.
Published online 13 November 2013.

1. Morris, G. P. & Allen, P. M. How the TCR balances sensitivity and specificity for the recognition of self and pathogens. *Nature Immunol.* **13,** 121–128 (2012).
2. Cheroutre, H. & Lambolez, F. The thymus chapter in the life of gut-specific intra epithelial lymphocytes. *Curr. Opin. Immunol.* **20,** 185–191 (2008).
3. Stritesky, G. L., Jameson, S. C. & Hogquist, K. A. Selection of self-reactive T cells in the thymus. *Annu. Rev. Immunol.* **30,** 95–114 (2012).
4. Fu, G. *et al.* Themis controls thymocyte selection through regulation of T cell antigen receptor-mediated signaling. *Nature Immunol.* **10,** 848–856 (2009).

5. Johnson, A. L. *et al. Themis* is a member of a new metazoan gene family and is required for the completion of thymocyte positive selection. *Nature Immunol.* **10,** 831–839 (2009).
6. Lesourne, R. *et al.* Themis, a T cell-specific protein important for late thymocyte development. *Nature Immunol.* **10,** 840–847 (2009).
7. Patrick, M. S. *et al.* Gasp, a Grb2-associating protein, is critical for positive selection of thymocytes. *Proc. Natl Acad. Sci. USA* **106,** 16345–16350 (2009).
8. Kakugawa, K. *et al.* A novel gene essential for the development of single positive thymocytes. *Mol. Cell. Biol.* **29,** 5128–5135 (2009).
9. Brockmeyer, C. *et al.* T cell receptor (TCR)-induced tyrosine phosphorylation dynamics identifies THEMIS as a new TCR signalosome component. *J. Biol. Chem.* **286,** 7535–7547 (2011).
10. Lesourne, R. *et al.* Interchangeability of Themis1 and Themis2 in thymocyte development reveals two related proteins with conserved molecular function. *J. Immunol.* **189,** 1154–1161 (2012).
11. Paster, W. *et al.* GRB2-mediated recruitment of THEMIS to LAT is essential for thymocyte development. *J. Immunol.* **190,** 3749–3756 (2013).
12. Daniels, M. A. *et al.* Thymic selection threshold defined by compartmentalization of Ras/MAPK signalling. *Nature* **444,** 724–729 (2006).
13. Hogquist, K. A. *et al.* T cell receptor antagonist peptides induce positive selection. *Cell* **76,** 17–27 (1994).
14. Oh-Hora, M. *et al.* Dual functions for the endoplasmic reticulum calcium sensors STIM1 and STIM2 in T cell activation and tolerance. *Nature Immunol.* **9,** 432–443 (2008).
15. Mariathasan, S. *et al.* Duration and strength of extracellular signal-regulated kinase signals are altered during positive versus negative thymocyte selection. *J. Immunol.* **167,** 4966–4973 (2001).
16. Fischer, A. M., Katayama, C. D., Pages, G., Pouyssegur, J. & Hedrick, S. M. The role of erk1 and erk2 in multiple stages of T cell development. *Immunity* **23,** 431–443 (2005).
17. McNeil, L. K., Starr, T. K. & Hogquist, K. A. A requirement for sustained ERK signaling during thymocyte positive selection *in vivo*. *Proc. Natl Acad. Sci. USA* **102,** 13574–13579 (2005).
18. Lorenz, U. SHP-1 and SHP-2 in T cells: two phosphatases functioning at many levels. *Immunol. Rev.* **228,** 342–359 (2009).
19. Zhang, J. *et al.* Involvement of the SHP-1 tyrosine phosphatase in regulation of T cell selection. *J. Immunol.* **163,** 3012–3021 (1999).
20. Plas, D. R. *et al.* Cutting edge: the tyrosine phosphatase SHP-1 regulates thymocyte positive selection. *J. Immunol.* **162,** 5680–5684 (1999).
21. Carter, J. D., Neel, B. G. & Lorenz, U. The tyrosine phosphatase SHP-1 influences thymocyte selection by setting TCR signaling thresholds. *Int. Immunol.* **11,** 1999–2014 (1999).
22. Štefanová, I. *et al.* TCR ligand discrimination is enforced by competing ERK positive and SHP-1 negative feedback pathways. *Nature Immunol.* **4,** 248–254 (2003).
23. Rybakin, V. & Gascoigne, N. R. J. Negative selection assay based on stimulation of T cell receptor transgenic thymocytes with peptide-MHC tetramers. *PLoS ONE* **7,** e43191 (2012).
24. Bouillet, P. *et al.* BH3-only Bcl-2 family member Bim is required for apoptosis of autoreactive thymocytes. *Nature* **415,** 922–926 (2002).
25. Moran, A. E. *et al.* T cell receptor signal strength in T_{reg} and iNKT cell development demonstrated by a novel fluorescent reporter mouse. *J. Exp. Med.* **208,** 1279–1289 (2011).
26. Johnson, D. J. *et al.* Shp1 regulates T cell homeostasis by limiting IL-4 signals. *J. Exp. Med.* **210,** 1419–1431 (2013).
27. Dubois, P. C. *et al.* Multiple common variants for celiac disease influencing immune gene expression. *Nature Genet.* **42,** 295–302 (2010).
28. Trynka, G. *et al.* Dense genotyping identifies and localizes multiple common and rare variant association signals in celiac disease. *Nature Genet.* **43,** 1193–1201 (2011).
29. Sawcer, S. *et al.* Genetic risk and a primary role for cell-mediated immune mechanisms in multiple sclerosis. *Nature* **476,** 214–219 (2011).
30. Fu, G. & Gascoigne, N. R. J. Multiplexed labeling of samples with cell tracking dyes facilitates rapid and accurate internally controlled calcium flux measurement by flow cytometry. *J. Immunol. Methods* **350,** 194–199 (2009).

Acknowledgements We thank X. L. Chen and Y. Xing for technical advice. We thank J. Ampudia, S. Vallée, J. Hu and S. Feldstein for help, and the National Institutes of Health (NIH) Tetramer Core Facility for production of MHC-I tetramers. Supported by NIH grants AI073870, DK094173 and GM065230 to N.R.J.G., DP1OD006433 to H.C., GM100785 and AI070845 to K.S.; Wellcome Trust Grant GR076558MA to O.A., and by the National University of Singapore. J.C. was supported by a fellowship from the Spanish Ministerio de Ciencia e Innovacion (MICIIN), J.A.H.H. by the Irving S. Sigal Fellowship of the American Chemical Society and NIH training grant T32AI07244, and K.S. by The Leukemia & Lymphoma Society Scholar Award 1440-11. The content is solely the responsibility of the authors and does not necessarily represent the official views of the National Institute of Allergy and Infectious Diseases, the NIH, or other funding agencies. This is manuscript number 21592 from The Scripps Research Institute.

Author Contributions G.F., J.C., S.R., V.R., F.L., J.B., K.S. and J.A.H.H. performed experiments and analysed data; W.P. and O.A. performed initial experiments on Themis–SHP1/2 interaction, G.F. and N.R.J.G. designed the project with help and insight from W.P., O.A., H.C. and K.S.; G.F. and N.R.J.G. wrote the manuscript with help from the other authors.

Author Information Reprints and permissions information is available at www.nature.com/reprints. The authors declare no competing financial interests. Readers are welcome to comment on the online version of the paper. Correspondence and requests for materials should be addressed to N.R.J.G. (micnrjg@nus.edu.sg).

METHODS

Mice. *Themis*$^{-/-}$ mice (B6.129S-*Themis*^{tm1Gasc}) were produced at TSRI and are available from Jackson Laboratory (Stock 010919). C57BL/6 (Thy1.2^{+}CD45.2^{+}) mice were bred at TSRI. OT-I and OT-I *Tap1*$^{-/-}$ animals were obtained from S. Jameson and K. Hogquist and *Bim* knockout mice from L. Sherman. All experiments were performed in accordance with the guidelines of the Animal Care and Use Committee of TSRI.

Antibodies. Anti-CD3 (145-2C11), anti-CD4 (RM4.4, RM4.5 and GK1.5), anti-CD8α (53-6.7), anti-CD8β (H35−17.2)) and anti-Vα2 (B20.1) were from eBioscience or Biolegend. Antibodies against phosphorylated extracellular signal-regulated kinase 1 and 2 (ERK1/2) (T^{202}/Y^{204}, catalogue no. 9101), phosphorylated PLC-γ1 (catalogue no. 2821), phosphorylated LAT (catalogue no. 3584), phosphorylated SHP1 (catalogue no. 8849), VAV (catalogue no. 2502), and NFATC2 (also known as NFAT1) (catalogue no. 5861) were from Cell Signaling Technology. Anti-phosphorylated tyrosine (4G10, catalogue no. 05-1050) and rabbit anti-Themis antibody were from Millipore (catalogue no. 06-1328). Anti-SHP1 antibody was from Santa Cruz Biotechnology (sc-287). Phospho-Src family (Tyr416) antibody (Cell Signaling catalogue no. 2101) cross-reacts with other Src-family kinases phosphorylated at the activating site. As a result probing thymocyte lysates with this monoclonal antibody shows phosphorylated forms of both p56 Lck and p59 Fyn.

Ca^{2+} flux. Ca^{2+} flux measurement by flow cytometry was performed as previously described[30]. Thymocytes from *Themis*$^{+/+}$ or *Themis*$^{-/-}$ OT-I *Tap1*$^{-/-}$ 4–6-week-old mice, both sexes, were used. Briefly, thymocyte suspensions were prepared, put in separate tubes and rested 3 h at 37 °C before assay. One of the two cell types was loaded for 5 min at room temperature with indodicarbocyanine (Cy5; 1 mg ml^{-1}) or was mock treated, followed by washing. Equal numbers of Cy5-labelled cell populations were mixed with the unlabelled sample; for example, OT-I *Tap1*$^{-/-}$*Themis*$^{+/+}$ (mock) plus OT-I *Tap1*$^{-/-}$*Themis*$^{-/-}$ (Cy5). Cells were suspended at a density of 2×10^6–6×10^6 cells per ml in cRPMI (RPMI medium supplemented with 10% (v/v) FCS, 100 U ml^{-1} of penicillin, 10 mg ml^{-1} of streptomycin, 292 mg ml^{-1} of glutamine, 50 mM 2-mercaptoethanol and 25 mM HEPES, pH 7.3) and were incubated for 30 min at 37 °C in 5% CO_2 with the calcium indicator Indo-1-AM (2 mM; Molecular Probes). Cells were washed twice with cRPMI. For antibody stimulation, cells were stained for 20 min on ice with biotin-conjugated anti-CD3 and anti-CD4 (RM4.4), as well as PerCP–Cy5.5-conjugated anti-CD8α and phycoerythrin (PE)-conjugated anti-CD4 (GK1.5) in cRPMI. Cells were washed once with cRPMI and once with cHBSS (Ca^{2+}-free and Mg^{2+}-free Hank's balanced-salt solution supplemented with 1% (v/v) FCS, 1 mM $MgCl_2$, 1 mM EGTA and 10 mM HEPES, pH 7.3) and were resuspended in cHBSS. Cells were prewarmed to 37 °C before analysis and were kept at 37 °C during event collection on an LSR II (Becton Dickinson). For cell stimulation, streptavidin (10 mg ml^{-1}; Jackson ImmunoResearch) was added to crosslink biotinylated antibodies; alternatively, cells were stimulated with tetramers (NIH tetramer core facility). $CaCl_2$ (2 mM) was added during analysis. Mean fluorescence ratio was calculated with FlowJo (TreeStar).

Imaging of Ca^{2+} flux. Knockout cells were prepared and pre-labelled with Cy5 as above[30] then both wild-type and knockout cells were mixed and loaded with 2 μM Ca^{2+}-sensitive dye Fluo-4. After washing in Ca^{2+}/Mg^{2+}-free medium with 1 mM EGTA, cells were mixed and added to the 37 °C imaging chamber containing either the antigen-presenting lipid bilayer or peptide-loaded RMA-S cells. After allowing cells to settle and starting imaging, 1 volume of pre-warmed medium containing 2.5 mM $CaCl_2$ and 2.5 mM $MgCl_2$ was added so that Ca^{2+} influx started at $t = 0$.

p-ERK analysis. For intracellular staining of phosphorylated ERK, stimulated cells were fixed with 4% paraformaldehyde for 12 min at room temperature and then plated in microtitre tubes (for phospho-flow analysis) or in poly-L-lysine-coated LabTek II chambers (for imaging). Cells were permeabilized with 0.3% Triton X-100 for 3 min at room temperature. Cells were then blocked with 5% normal goat serum and incubated with rabbit monoclonal antibody against phospho-ERK, after which they were incubated with Alexa Fluor 488-conjugated Fab fragments against rabbit antibodies (Molecular Probes) for secondary detection (either phospho-flow or microscopy). For flow cytometry analysis, one of the two cell types were pre-labelled with dye Cy5 and the other one was mock labelled. Then the two cell types were mixed in 1:1 ratio and processed for stimulation and staining. Phospho-flow analysis of p-ERK was done on a BD LSR-II digital flow cytometer and the two cell types were distinguished by Cy5 labelling. p-ERK imaging was done as described previously with modification[31]. Briefly, after intracellular staining of p-ERK, nuclei were counterstained with the DNA binding dye 4′,6-diamidino-2-phenylindole (DAPI, Invitrogen). All images were captured with a Zeiss Axiovert 200 M inverted microscope. SlideBook software (Intelligent Imaging Innovations) was used for the capture as well as for deconvolution and image analysis, and ImageJ was used for image presentation.

NFATC2 imaging. Nuclear translocation of NFATC2 (NFAT1) was imaged as described above regarding p-ERK imaging[31], and analysed using CellProfiler software (Broad Institute).

Immunoprecipitation and western blotting analysis. Briefly, cells were stained with antibodies against CD3 and CD4 or tetramers on ice for 15 min and stimulated by rapidly warming to 37 °C with pre-warmed PBS for indicated times. Cells were then lysed and processed for immunoprecipitation or immunoblot analysis as described in detail in ref. 32. In some cases, after primary antibody incubation, membranes were incubated with goat anti-rabbit IgG (H+L), DyLight 800-conjugated (Pierce, catalogue no. 35571) or goat anti-mouse IgG (H+L), DyLight 680-conjugated (Pierce, catalogue no. 35519), and detected and quantified with a LiCor Odyssey infrared imaging system. Human embryonic kidney epithelial cells (HEK293), which express SHP2 but little SHP1[33,34], were transfected by calcium phosphate precipitation and lysates prepared as described[11]. Streptactin-Sepharose beads (IBA BioTAGnology) were used for THEMIS-Strep pull-downs, after which beads were washed three times with lysis buffer. Bound proteins were eluted with 5 mM biotin and subjected to SDS–PAGE[11].

***In vitro* apoptosis assay.** Experiments were performed as described previously[23]. Briefly, pre-selection thymocytes were stimulated with the various tetramers for 17 h. Apoptosis was determined by staining active caspase-3 with fluorescein isothiocyanate (FITC)-conjugated specific antibody following the manufacturer's protocol (APO ACTIVE 3 detection kit, Cell Technology, catalogue no. FAB200-1), and analysed by FACS.

Phenotyping of agonist-selected T cells. Agonist-selected T cells were analysed in bone marrow reconstituted mice. Briefly, *Themis*$^{+/+}$ (CD45.1^{+}/CD45.2^{+}) and *Themis*$^{-/-}$ bone marrow cells (CD45.2^{+}) were mixed 1:1 and injected into lethally irradiated (2 × 5.5 Gy, separated by 3–4 h) B6 recipient mice (CD45.1^{+}). At various times post bone marrow reconstitution, tissues and organs of recipient mice were collected and relevant T-cell subsets were analysed. Splenocytes, IELs and liver mononuclear cells were prepared as previously described[35,36]. Cells were suspended in PBS + 5% FCS + 0.16% azide and anti-CD16/CD32 (2.4G2) Fc-receptor antibody (BD Biosciences) was used to block Fc-antibody binding. The following antibodies were purchased from BD Biosciences: TCRγδ-FITC (GL3), TCRβ-APC-ef780 (H57-597), NK1.1-FITC (PK136), CD8α-PE (53-6.7), CD8β-FITC (53-5.8), CD19-APC (1D3), CD45.2-PercP-Cy5.5 (104). The following antibodies were purchased from eBioscience: CD4-eF450 (RM4-5), CD5-ef450 (53-7.3), CD45.1-PE-Cy7 (A20), CD69-eF450 (H1.2F3), CD90.2-APC (53-2.1). The following antibodies were purchased from Invitrogen: CD8α-PO (5H10). The following antibodies were purchased from Caltag: CD4-PO (RM4-5). All antibodies were directly conjugated to fluorophores. An LSR II cell analyser (BD Biosciences) was used for the flow cytometry, and FlowJo software (TreeStar) was used for analysis.

Statistical testing. Statistics were performed as described in Figure legends using Excel, GraphPad Prism, or Igor Pro (Wavemetrics).

31. Fu, G. *et al.* Protein kinase C η is required for T cell activation and homeostatic proliferation. *Sci. Signal.* **4,** ra84 (2011).
32. Huang, Y. H. *et al.* Positive regulation of Itk PH domain function by soluble IP4. *Science* **316,** 886–889 (2007).
33. Minoo, P., Zadeh, M. M., Rottapel, R., Lebrun, J. J. & Ali, S. A novel SHP-1/Grb2-dependent mechanism of negative regulation of cytokine-receptor signaling: contribution of SHP-1 C-terminal tyrosines in cytokine signaling. *Blood* **103,** 1398–1407 (2004).
34. Simoneau, M. *et al.* Activation of Cdk2 stimulates proteasome-dependent truncation of tyrosine phosphatase SHP-1 in human proliferating intestinal epithelial cells. *J. Biol. Chem.* **283,** 25544–25556 (2008).
35. Hammond, K. J. *et al.* CD1d-restricted NKT cells: an interstrain comparison. *J. Immunol.* **167,** 1164–1173 (2001).
36. Gangadharan, D. *et al.* Identification of pre- and postselection TCRαβ^{+} intraepithelial lymphocyte precursors in the thymus. *Immunity* **25,** 631–641 (2006).
37. Hogquist, K. A., Jameson, S. C. & Bevan, M. J. Strong agonist ligands for the T cell receptor do not mediate positive selection of functional CD8^{+} T cells. *Immunity* **3,** 79–86 (1995).
38. Hogquist, K. A. *et al.* Identification of a naturally occurring ligand for positive selection. *Immunity* **6,** 389–399 (1997).
39. Santori, F. R. *et al.* Rare, structurally homologous self-peptides promote thymocyte positive selection. *Immunity* **17,** 131–142 (2002).
40. Rosette, C. *et al.* The impact of duration versus extent of TCR occupancy on T cell activation: a revision of the kinetic proofreading model. *Immunity* **15,** 59–70 (2001).
41. Huang, J. *et al.* The kinetics of two-dimensional TCR and pMHC interactions determine T-cell responsiveness. *Nature* **464,** 932–936 (2010).
42. Alam, S. M. *et al.* T cell receptor affinity and thymocyte positive selection. *Nature* **381,** 616–620 (1996).
43. Alam, S. M. *et al.* Qualitative and quantitative differences in T cell receptor binding of agonist and antagonist ligands. *Immunity* **10,** 227–237 (1999).
44. Juang, J. *et al.* Peptide-MHC heterodimers show that thymic positive selection requires a more restricted set of self-peptides than negative selection. *J. Exp. Med.* **207,** 1223–1234 (2010).

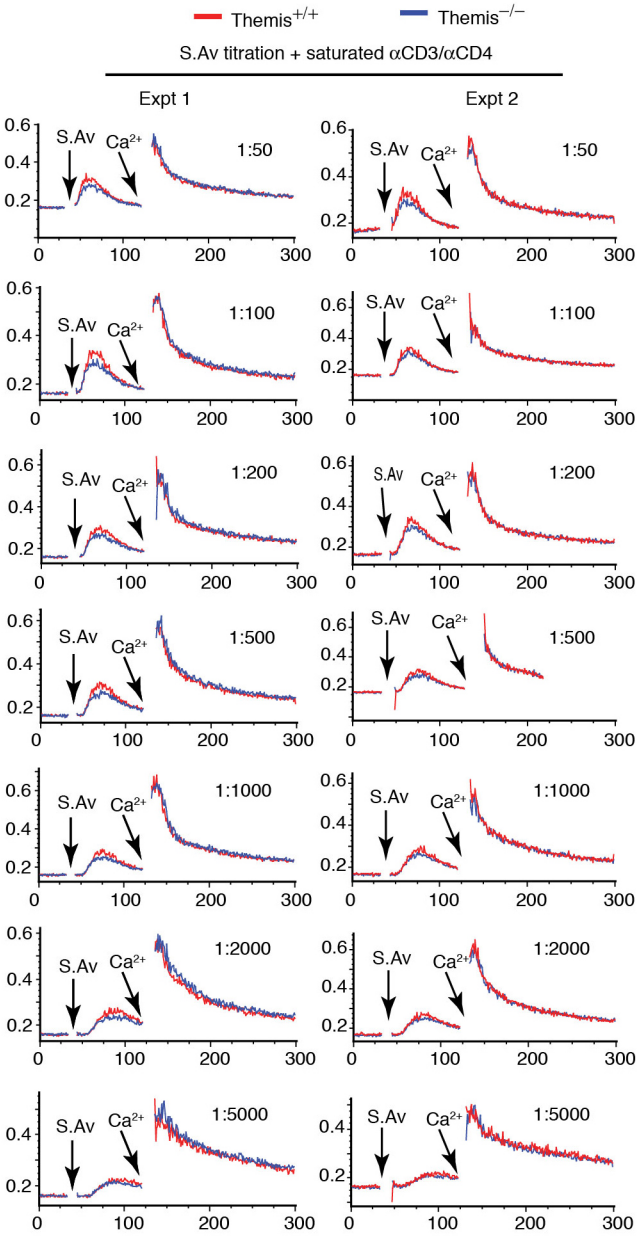

Extended Data Figure 1 | Ca^{2+} flux in Themis-deficient thymocytes stimulated by TCR crosslinking. Thymocytes from wild-type or Themis-deficient mice were first stained with saturated amount of anti-CD3/CD4 antibodies and subsequently cross-linked with titrated amount of streptavidin (S.Av). Two independent experiments are shown here.

a

Peptide	Sequence	Activation of mature T cells	FTOC selection (OT-I β2$m^{-/-}$ or *Tap1*$^{-/-}$)	Relative potency (CD69 upregulation)	A_cK_a (2D affinity) (μm^4)	K_d (3D affinity) (μM)	Tetramer avidity (nM)
OVA	SIINFEKL	Strong agonist	Negative selection	1	1 x 10^{-3}	5.9	4
A2	SAINFEKL	Strong agonist	Agonist/negative selection		7 x 10^{-4}	4.4	
Q4	SIIQFEKL	agonist	Agonist/negative selection	39			29
Q4R7	SIIQFERL	agonist	Agonist/negative selection	81			48
Q4H7	SIIQFEHL	Agonist/antagonist	Positive selection	167			51
Q7	SIINFEQL	Agonist/antagonist	Positive selection	268			
G4	SIIGFEKL	Agonist/antagonist	Positive selection	7,515	2 x 10^{-5}	10.0	
E1	EIINFEKL	Antagonist	Positive selection	56,524	5 x 10^{-6}	22.6	
Catnb	RTYTYEKL	Not measurable	Positive selection			136 (10°C)	
Cappa1	ISFKFDHL	Not measurable	Very weak pos. sel^{n}			211 (10°C)	
P815 or VSV	HIYEFPQL RGYVYQGL	Not measurable	Not measurable	∞	< 10^{-8}	not measurable	
Refs.			12, 13, 37-40	12	41	40, 42-44	12

b

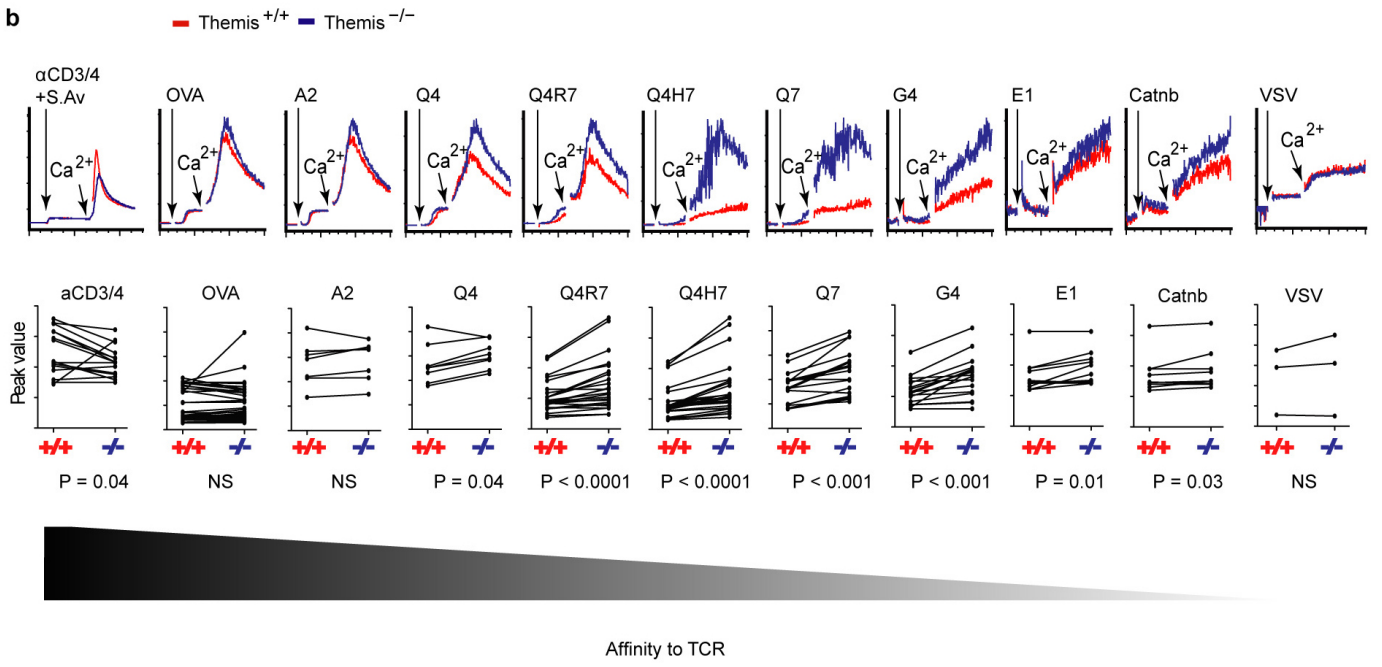

Extended Data Figure 2 | OT-I TCR system and comparison of Ca^{2+} flux between Themis-sufficient and Themis-deficient pre-selection thymocytes. **a**, Summary of responses of OT-I T cells and thymocytes to different peptides. Data from references 12, 13 and 37–44. **b**, Representative FACS plots from Fig. 1a are shown here again for illustration (top panel), statistical analysis of Ca^{2+} flux between Themis-sufficient (+/+) and Themis-deficient (−/−) thymocytes were calculated using Wilcoxon signed rank test (*P* value listed), each line links cells from a pair of mice being compared in the same tube as described[30] (bottom panel). Results are pooled from multiple experiments as described in Fig. 1 legend.

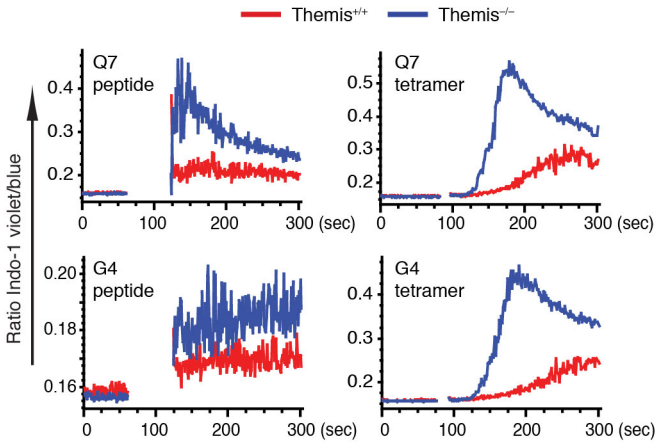

Extended Data Figure 3 | Comparison of Ca^{2+} flux induced by different methods. Thymocytes from indicated mice were either stimulated with peptide presented on thymocytes themselves (left) or with K^b-tetramers (right). As shown, similar results were obtained by both stimulation methods.

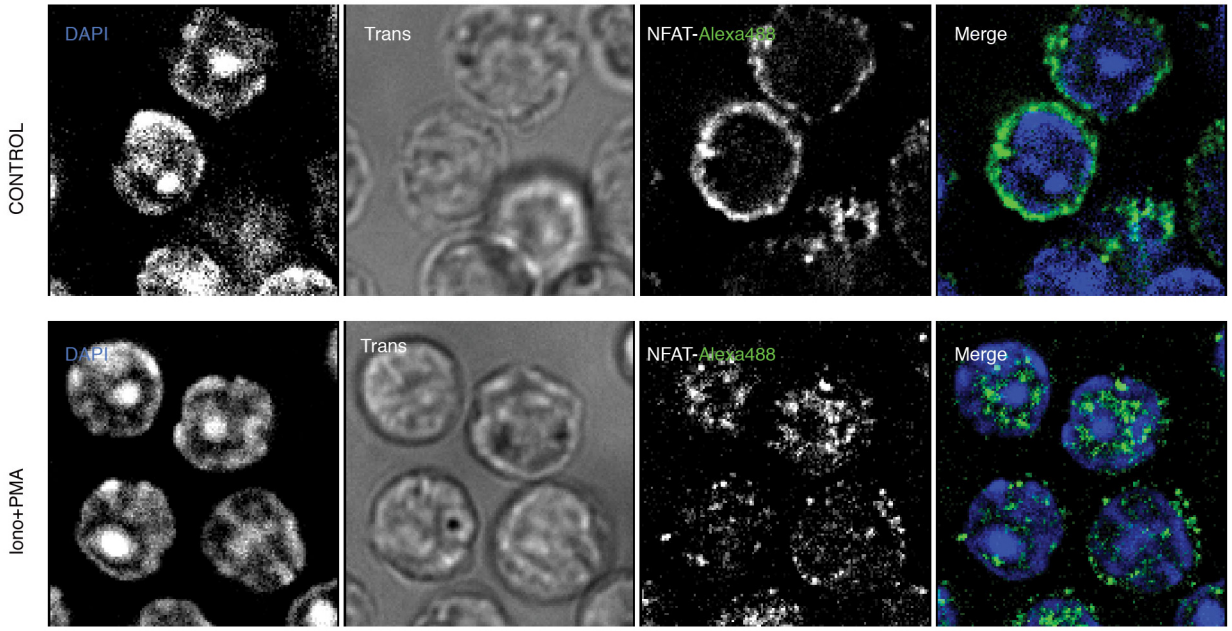

Extended Data Figure 4 | Quantification of NFATC2 nuclear translocation. Thymocytes were stimulated with ionomycin/PMA (phorbol-12-myristate-13-acetate) (Iono+PMA) to obtain maximal extent of NFATC2 nuclear translocation as a positive control for image analysis. NFATC2 translocation in non-stimulated cells (CONTROL) is used as negative control for image analysis. DAPI and NFATC2 staining are colour-coded as indicated.

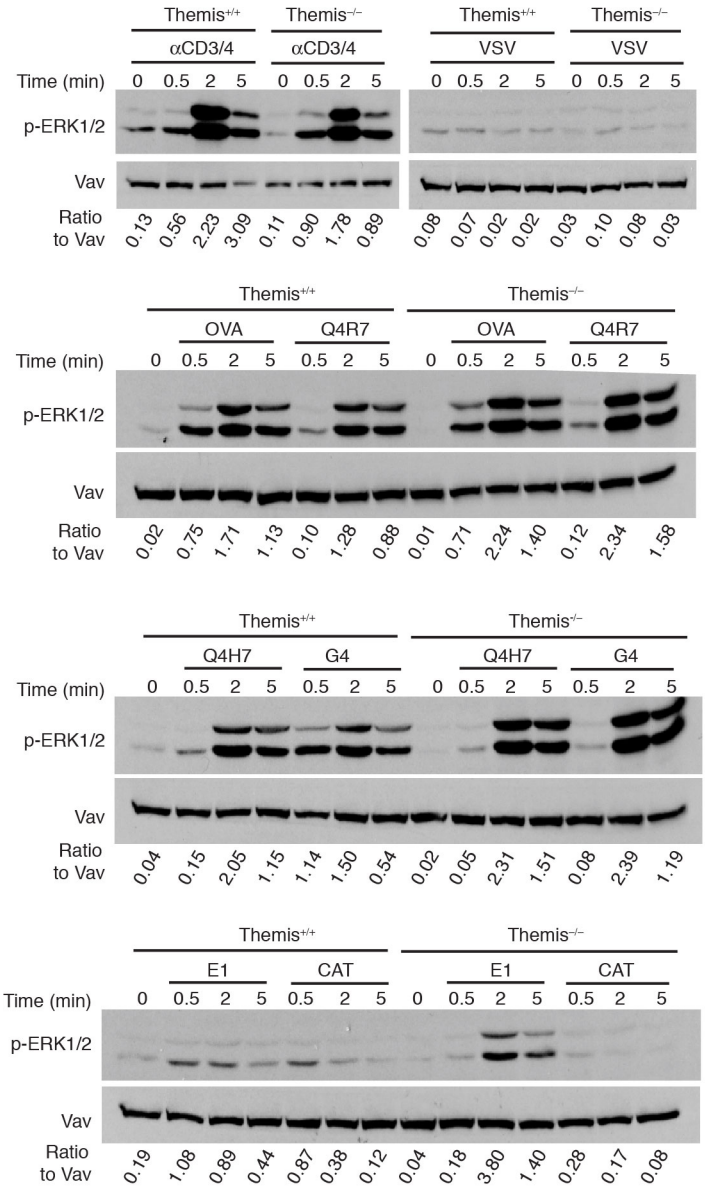

Extended Data Figure 5 | Biochemical analyses of ERK phosphorylation in Themis-deficient thymocytes. ERK1 and 2 phosphorylation of indicated thymocytes in response to different stimuli, normalized to VAV. Representative of 4 experiments.

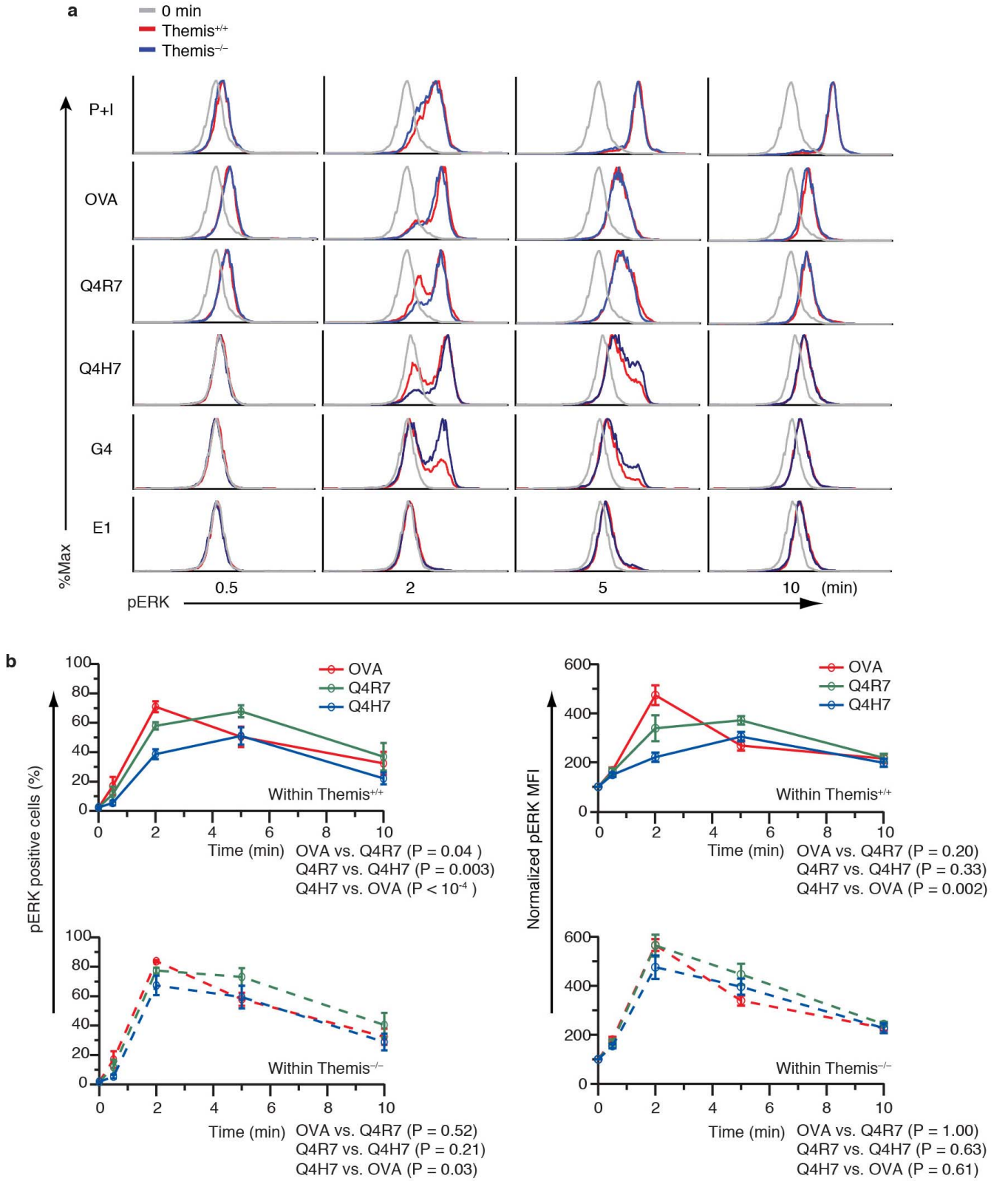

Extended Data Figure 6 | Flow-cytometric analysis of ERK phosphorylation. Thymocytes were prepared and stimulated with K^b-tetramers. Representative FACS plots are shown in **a**. Data compiled from several experiments. PMA and ionomycin (P+I) treatment was used as a positive control for stimulation to obtain maximal ERK phosphorylation. **b**, Same p-ERK data as in Fig. 2b, presented as responses to the different ligands overlaid within the same mouse genotype.

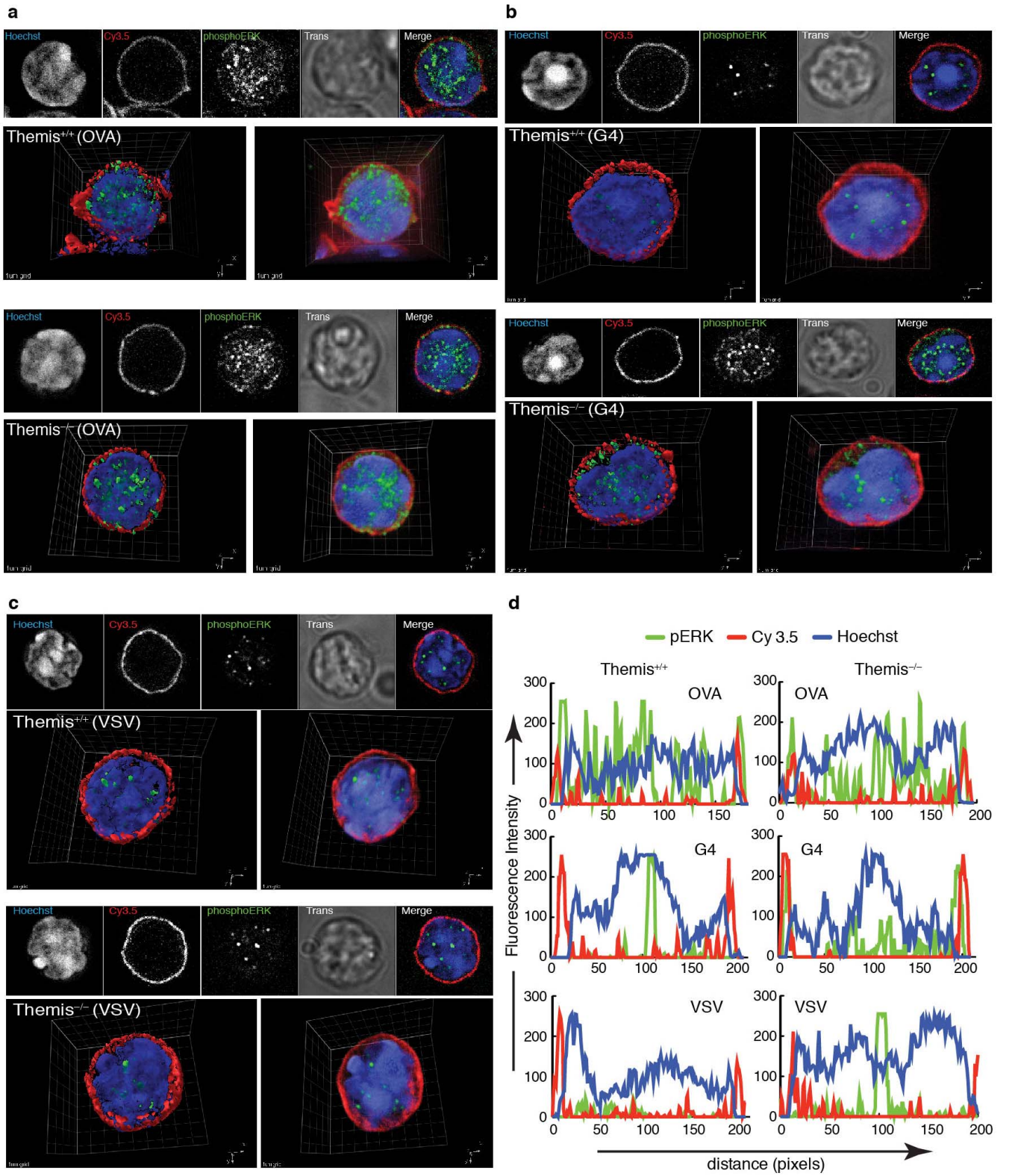

Extended Data Figure 7 | Three-dimensional reconstruction images of negative-selection-like ERK signalling in *Themis*$^{-/-}$ thymocytes in response to positive-selecting ligands. a–c, *Themis*$^{+/+}$ or *Themis*$^{-/-}$ OT-I *Tap1*$^{-/-}$ pre-selection thymocytes were stimulated with K^b–OVA (**a**), K^b–G4 (**b**) or K^b–VSV (**c**). Localization of p-ERK was determined by specific staining with anti-p-ERK antibody. Nuclei were counterstained with Hoechst 33342, and plasma membrane was labelled with Cy3.5. Top panels represent each separate channel of a single centred plane. Bottom panels represent two different 3D reconstructions of 30 planes (step = 0.2 μm), surface rendering (left) and volume rendering (right). **d**, Fluorescence line profile analysis of representative cells in **a**, **b** and **c**, green line (p-ERK) blue line (Hoechst) and red line (Cy3.5).

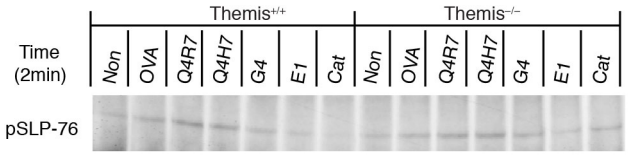

Extended Data Figure 8 | SLP-76 phosphorylation is not affected in Themis-deficient thymocytes. Phosphorylation of SLP-76 was determined in cell lysates. Representative of 2 experiments.

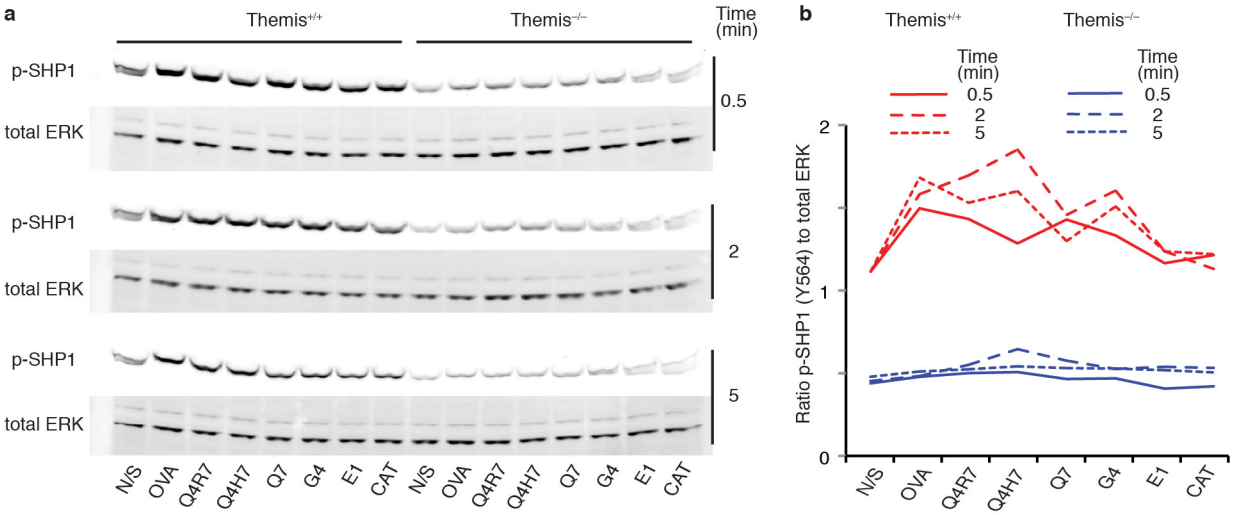

Extended Data Figure 9 | Decreased SHP1 phosphorylation in *Themis*$^{-/-}$ double-positive cells. a, Phosphorylation of SHP1 was determined in cell lysates. In this experiment, cell lysates from the same time point after stimulation (0.5, 2 and 5 min , respectively) were grouped together and directly compared on the same gel. **b**, Quantitation: the intensity ratio of p-SHP1 to total ERK was determined by LiCor Odyssey software.

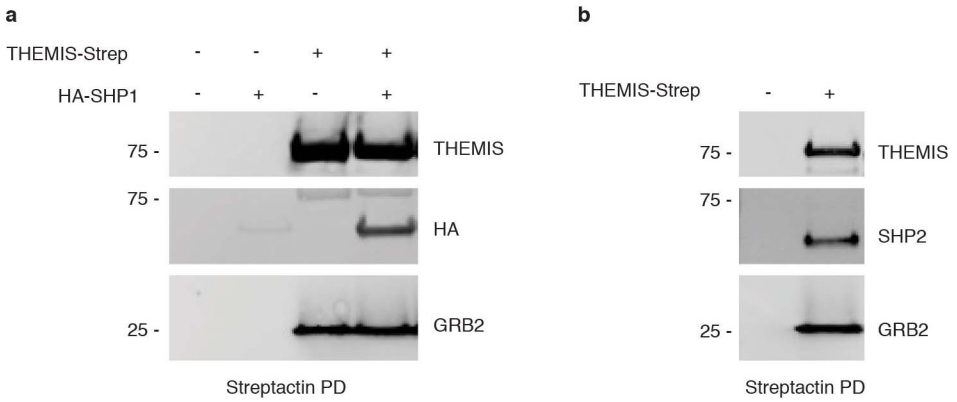

Extended Data Figure 10 | THEMIS forms complexes with SHP1 and SHP2. HEK293 cells were transiently transfected with the indicated expression vectors. **a**, **b**, Pull-down assays using Streptactin beads were performed two days after transfection and the precipitate subjected to SDS–PAGE and immunoblotting with anti-haemagglutinin (HA) tag (**a**) and anti-SHP2 (**b**) antibodies, respectively. Representative of 3 (**a**) and 2 (**b**) similar experiments, respectively. Note that HEK293 cells express SHP2 but little SHP1. Cells originally from ATCC, tested negative for mycoplasma within previous 3 months, not short tandem repeat profiled. Constitutive binding of GRB2 to THEMIS has been reported previously.